

EL/PL system optimization and image calibration for different PV devices

R. P. Roodt*

E. E. van Dyk, J. L. Crozier McClelland, R. M. Dix-Peek

Department of Physics, Nelson Mandela University

*s217357709@mandela.ac.za

Abstract

Electroluminescence (EL) and Photoluminescence (PL) imaging of Photovoltaic (PV) devices are well known qualitative and quantitative, non-destructive characterization techniques. The quality of an image is important in luminescence image quantification. Aside from basic optical optimisation (such as focus, relative position, lens distortion and contrast), a camera's sensor's properties can affect an image's quality. In literature, a process has been developed to corrected for these factors when capturing EL and PL images of silicon PV devices. This procedure however has not been investigated to see if it also works for other PV materials, such as perovskite, Multi-junction III-V concentrator cells, etc. It is therefore necessary to further develop this process and investigate it for other PV devices, as it would be different for each material's luminescence spectrum. This study illustrates how the process is investigated and used in correcting images acquired for Silicon, Multi-junction III-V concentrator cells, and perovskite.

Keywords : Luminescence Imaging, Photovoltaic devices, image calibration.

1. Introduction

The demand of renewable energy globally has increased significantly to achieve net zero emission goals(Bojek, 2022). Specifically, the increase in the dependence on Photovoltaic devices to produce electricity. This pushed for the development of new solar cell technologies, to improve on the efficiency of the solar panels(Bojek, 2022). To understand and improve upon the solar cell technologies, characterisation needs to take place. Electroluminescence (EL) imaging is a fast and non-destructive technique used for spatially resolved characterisation of Photovoltaic (PV) devices. It is shown to be suitable for quantitative analysis, the identification of cracks, broken fingers, shunts, and interconnects(Breitenstein *et al.*, 2016). Quantitative analysis of solar cells, such as local voltage and series resistance mapping and the effective diffusion length are also possible using EL imaging(Trupke *et al.*, 2007; Würfel *et al.*, 2007) . Another technique that compliments EL imaging is Photoluminescent (PL) imaging.

Before using EL and PL images for obtaining the above-mentioned properties, image correction is required due to optical and sensor related properties which distort the image, which reduces its clarity. A routine was developed by Karl Bedrich (Bedrich *et al.*, 2016) for correcting the distortion in silicon CCD camera when imaging Silicon PV devices. Using a Silicon CCD camera has the advantage of being faster and has much higher image resolution compared to InGaAs Cameras, but the InGaAs sensor has a much higher relative external quantum efficiency at the wavelength spectrum emitted by Si PV cells(Mitchell *et al.*, 2012). The silicon sensor can only capture a small portion of the emission spectrum.

The objective of this research is to investigate how this procedure works when applied to different PV devices using the same CCD sensor and to look at how the point spread function evolves for each PV device's specific wavebands.

2. Theory

2.1.EL and PL

EL is the luminescence seen when the excitation of carriers is caused by injecting current into the sample. PL on the other hand is the luminescence observed when the carriers within

a semiconductor are excited due to photon absorption solid state electronic devices (Streetman, 1995).

2.2. The Image correction routine

In this section the EL Image correction procedure is discussed with each step of the correction procedure described with examples shown.

The routine is:

- Focusing the camera
- Image correction by:
 - Removing Single time effects (STE)
 - Dark Current removal
 - Artifact removal
 - Deconvolution using a point spread function (PSF)
 - Perspective correction.

2.2.1. Single time effects

STE are caused by cosmic high energy radiation interacting with the CCD array of the camera. They are seen as small spots in an EL image. The likeliness of seeing STE increase with increasing exposure time and decreasing junction voltage of the PV device (Bedrich *et al.*, 2016). Due to the randomness of these effects, the possibility of them occurring twice in the same spot is minuscule. Therefore, to correct the EL image for these STE, at least two or more EL images needs to be taken under the same conditions. A threshold filter is then applied to each pixel using the multiple EL images. Figure 1.a) illustrates an EL image that has STE, the bright spots that are circled, and Figure 1.b) shows that same EL image after applying the filter to remove those STE's.

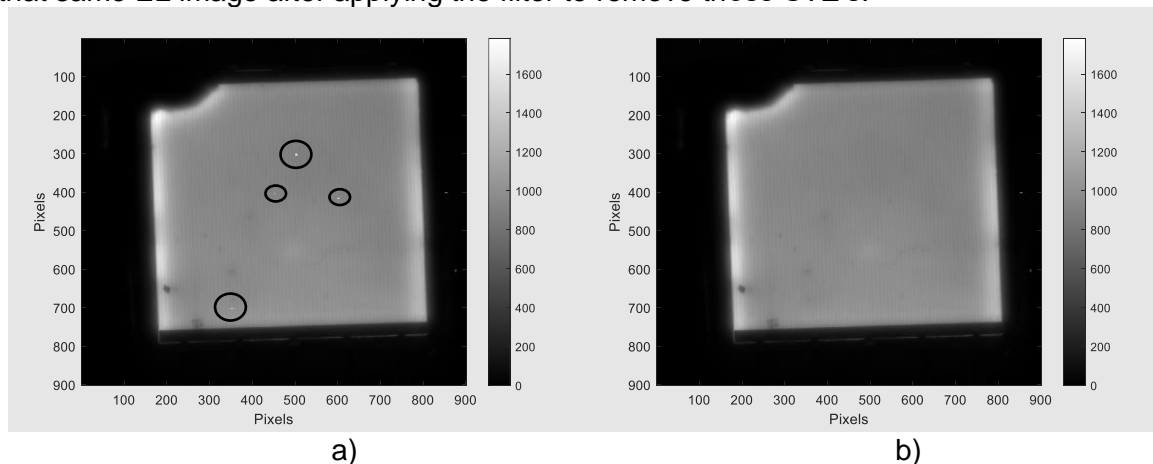


Figure 1. a) An EL image having STE. b) The image after removing the STE.

2.2.2. Dark Current correction

Removing dark current (thermal noise and defective pixels) and environmental light, is usually done by subtracting an EL image from an image taken under the same circumstances, the same system and exposure time, as the EL image but the PV Device is at open circuit, no external current is being injected into the sample (Bliss *et al.*, 2015). The dark current image can be seen in Figure 2.a) and Figure 2.b) is what results when subtracting Figure 2.a) from Figure 1.b).

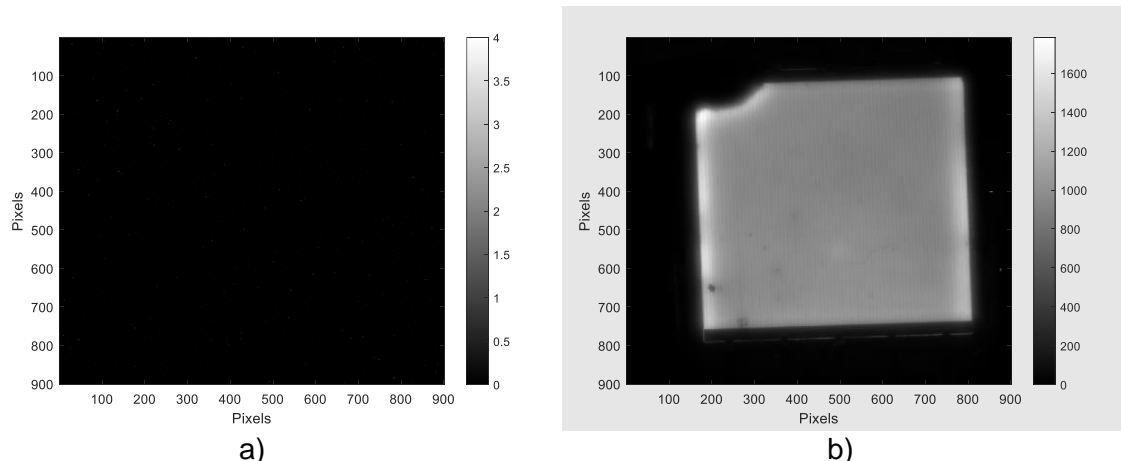


Figure 2. a) Dark Current image. b) EL image after removing the dark current image.

2.2.3. Artifact removal

After removing the STE and the dark current correction, there still might be artifacts visible in the images. These artifacts are caused by defective pixels within the CCD array. These artifacts can be removed by using a median filter (Bedrich *et al.*, 2016). In Figure 3.a) the artifacts are highlighted by boxes around them. Applying the median filter to this image results in Figure 3.b)

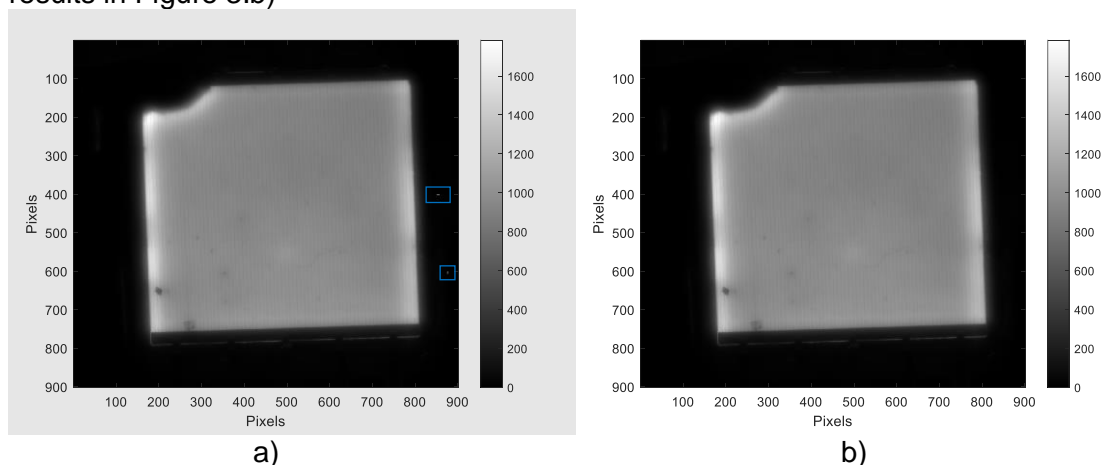


Figure 3. a) EL image having artifacts. b) Resulting EL image after applying the median filter.

2.2.4. Deconvoluting image with point spread function

Numerous events contribute to the blurring of EL and PL images, such as diffraction, chromatic aberration, photon scattering within the CCD sensor and light trapping, just to name a few. However, considering the nature of these optical artefacts, the image can be deconvoluted by making use of an optimised PSF and the appropriate algorithm (Payne *et al.*, 2016). This will increase the sharpness of the image. A point spread function is looking at how the light generated by a point source spreads out in the detector, Figure 4. a) is an example of a PSF. Figure 4.b) is a three-dimensional view of the PSF shown in Figure 4.a). It was found that the PSF is wavelength dependent. Therefore, the PSF needs to be obtained for each PV technology for a given optical setup. Different methods have been used to find the PSF, but the most promising method is by directly measuring it. This is done by covering the PV device with opaque material with a pinhole. This is done to prohibit any light from passing through except at the pinhole. There are various deconvoluting methods, but the Richardson-Lucy deconvolution method is the most often used. Karl Bedrich had numerous pinholes, 147 to be exact, covering his PV module and averaged all the PSF's to obtain the PSF he used in his deconvoluting process (Bedrich *et al.*, 2016; Payne *et al.*, 2016). The PSF obtained in EL images can also be used in the Deconvolution of PL images

as there is only a small shift in the wavelength, due to the method of PL adding thermal energy to the material(Hameiri *et al.*, 2015).

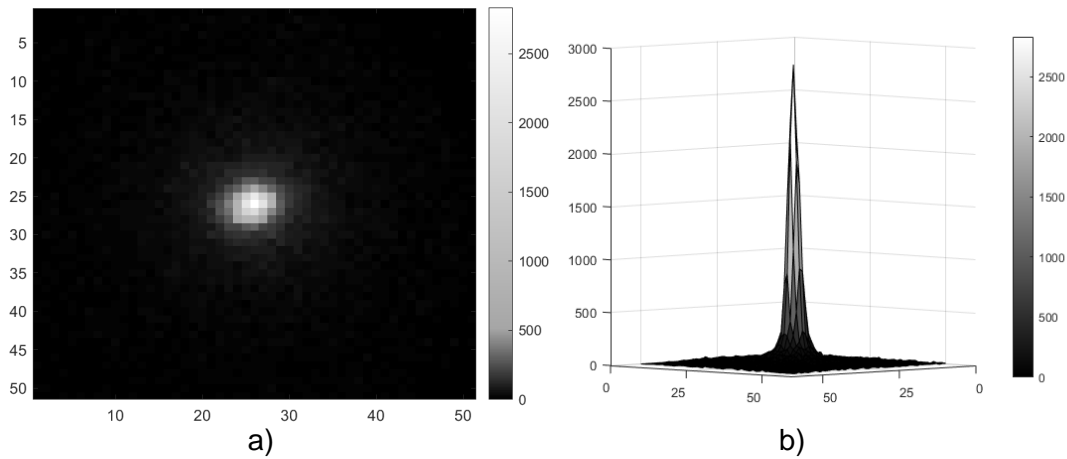


Figure 4. a) a PSF image. b) a 3-D view of the PSF

2.2.5. Perspective correction

Correcting the perspective of the PV device to align with the image corners is essential for image comparison of a PV device over a period to investigate degradation and any features that might occur within the device. For example, Figure 5.a) is a section of the EL image in Figure 3.a). Some features are highlighted in Figure.

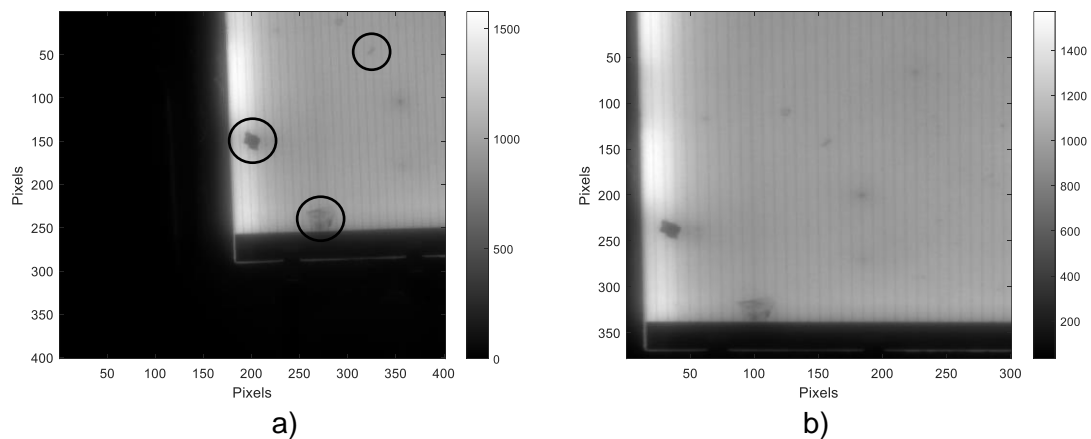


Figure 5. a) EL image before perspective correction and b) after perspective correction.

If this PV device should be placed in operation, and over a period the dark spot on the left edge should grow, one will then be able to identify it by using the perspective correction procedure and compare the image to Figure 5.a).

3. Research methodology

In this section the system and the method followed to acquire the results is discussed

3.1. System

The EL imaging system consists out of a Keithley 2450 Source meter and an acA5472-17um Basler ace camera. A LabVIEW program was used to communicate with the source meter and camera. The LabVIEW program allows the user to specify the current and voltage the source meter needs to supply the PV device, it also enables the user to modify the exposure time, and the gain of the camera.

3.2. Routine

Each PV device, namely, monocrystalline silicon concentrator, perovskite, and a Multi-junction III-V concentrator (InGaP – InGaAs - Ge) has different emission wavelengths. It was therefore necessary to isolate these emission wavelengths, shown in Figure 6., for each PV device by using the correct filter. For the silicon, the routine was done twice, once with the 950nm bandpass filter and the second time without it. This was done to see how the filter effects the image quality. For the perovskite, the routine was followed once with a 775nm bandpass filter as the perovskite only has one emission peak. For the III-V triple junction concentrator, the routine was followed twice. First for the top or first layer of the concentrator, InGaP, with a 675nm bandpass filter. The second time was for the second layer of the concentrator, which is InGaAs, making use of an 875nm bandpass filter. The bandwidth of all these filters is 50nm FWHM where the mentioned wavelength is the centre of the band.

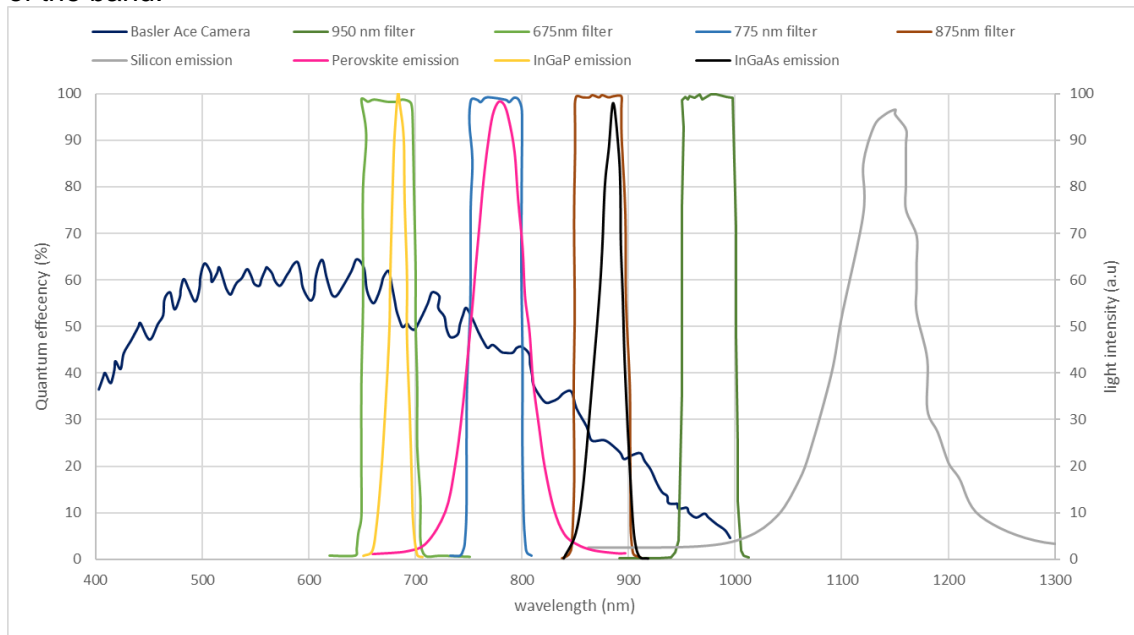


Figure 6. The emission peaks for the three PV devices.

The routine followed is discussed below.

3.2.1. Focusing the camera

For each PV device the current was set to the I_{sc} value of the device and the Keithley source meter supplied the necessary voltage. The exposure time and gain were varied until a vague image of the sample could be seen. Thereafter manual adjustment was made to the focus point of the lens until a clear contrast between the device and the background was seen.

3.2.2. Single time effects

To remove the STE, five images were taken consecutively under the same power, at I_{sc} , and camera settings. The standard deviation for each pixel was calculated and then averaged for the standard deviation across all the pixels. If the standard deviation of the pixel exceeded 3 times the average standard deviation, that pixel was then given the minimum value of that pixel in the five images.

3.2.3. Dark Current correction

For this the PV devices were imaged under open circuit, meaning no external current was supplied to the PV device. The same method described in section 3.1.2 was used to correct the dark current image. This image was then subtracted from the EL image obtained under I_{sc} conditions.

3.2.4. Artifact removal

MATLAB has a built in median filter function, `medfilt2`, and this was used to filter out artifacts.

3.2.5. Deconvoluting with point spread function

A black piece of vinyl re-enforced with paper, to give the pinhole structural integrity, was used to acquire images of the PSF. For consistency, the same black contact paper was used for obtaining the PSF of each of the PV devices. Once, again MATLAB assisted in correcting these images as it has a built in Lucy-Richardson deconvolution function that uses the PSF to correct the image.

3.2.6. Perspective correction

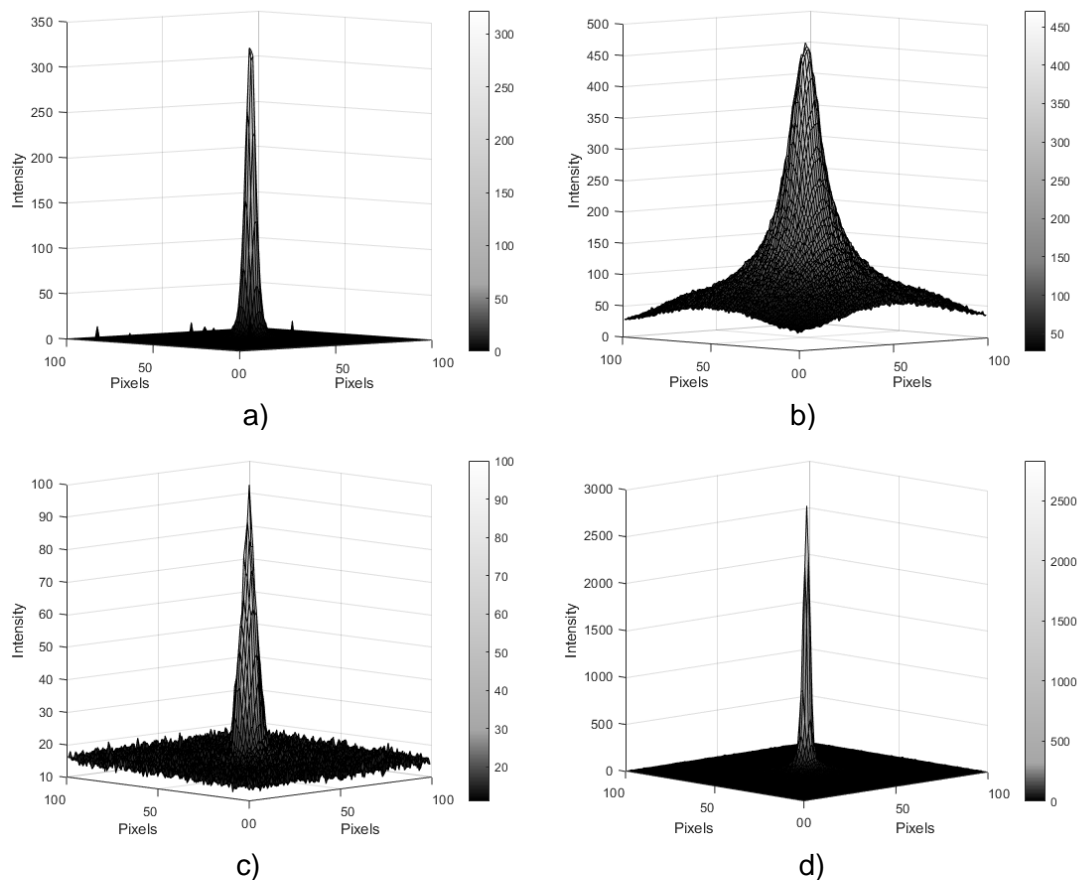
To correct the perspective of the image, a MATLAB script was written that allows the user to select the four corners of the PV device and it then aligns and crops the image to the size of the PV device.

4. Results

In the first part of the results the PSF's obtained for each PV device is showed and compared to one another. In the later part of this section the results obtained when applying the routine to the EL images is shown.

4.1.PSF

The PSF's obtained for each of the PV devices are shown in Figure 7.a) – e).



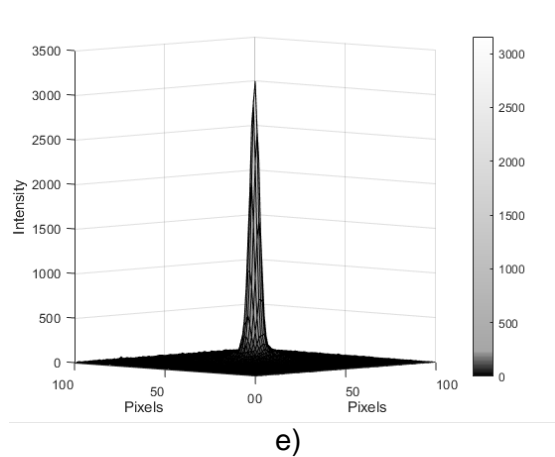


Figure 7. 3-D views of the PSF's obtained for the different PV devices: a) PSF for silicon using the 950nm filter, b) PSF for silicon without the filter, c) PSF for perovskite with 775nm filter, d) PSF for the top layer of the concentrator with 675nm filter and e) PSF for the second layer of the concentrator with 875nm filter.

Figure 7.a) is the PSF obtained for the silicon using the 950nm filter and Figure 7.b) is the PSF obtained for the silicon without a filter. Comparing both PSFs with each other we see that the peak intensity with the filter is less than that of without the filter. This makes sense as the filter only allows light through at the starting portion of the emission peak of silicon. Without the filter a wider range of the emission peak to be picked up and the PSF extends over a large number of pixels. When the filter is utilised, the PSF is narrower. Agreeing with the results seen by (Walter *et al.*, 2014).

Figure 7.c) is the PSF obtained for the perovskite device. Its intensity is much lower due to the black contact paper being placed over a low luminescence area of the sample. What is interesting to see is that there is a constant background noise around the peak of the PSF. This is being observed even with a filter in front of the lens. Figure 7.d) and e) is the PSFs obtained for the first and second layer of the Multi-junction III-V concentrator cell. Both have clear PSF with minimal background noise, but the broadness of the PSF for the second layer is wider, over more pixels, than that of the first layer. This follows theory as the PSF should cover a larger area for higher wavelengths as the mean free path within the silicon CCD increases for higher wavelengths(Breitenstein *et al.*, 2016).

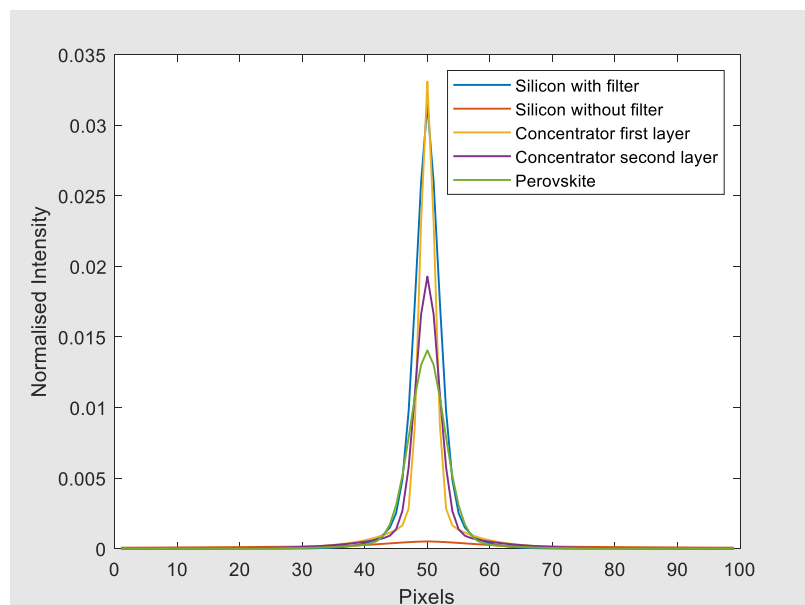


Figure 8. Normalised cross section of the PSFs for the different PV devices.

To use the PSFs illustrated in Figure 7 in the deconvolution function, they need to be normalized. This is done by dividing each pixel value by the sum of all the pixels. Figure 8. Illustrates a cross sectional view of the normalized PSFs for each PV device.

4.2. The routine

The results obtained when applying the image correction routine to EL images of the three PV devices is shown in this section. Figure 9. a) is the STE corrected EL image obtained for the silicon. Even though the STE have been corrected, artifacts can still be seen, the bright spots seen in the image. Applying the image correction procedure to this image results in Figure 9. b). The darker regions within the device do not appear clear even after correcting the image. This is likely due to the optics of this complete system (including device).

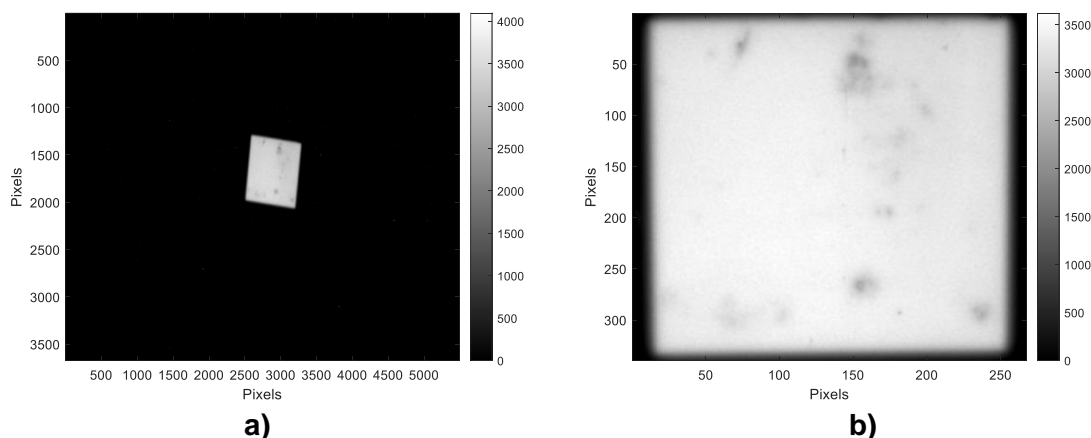


Figure 9. a) EL images of the silicon with the filter and b) the EL image after applying the correction routine.

The EL image captured for the silicon concentrator without the filter is shown in Figure 10.a). The corrected EL image is shown in Figure 10. b). Comparing this image to the one seen in Figure 9.b), its edges are not as sharp, and the darker spots are not as clear. This illustrates that using a filter result in clearer images.

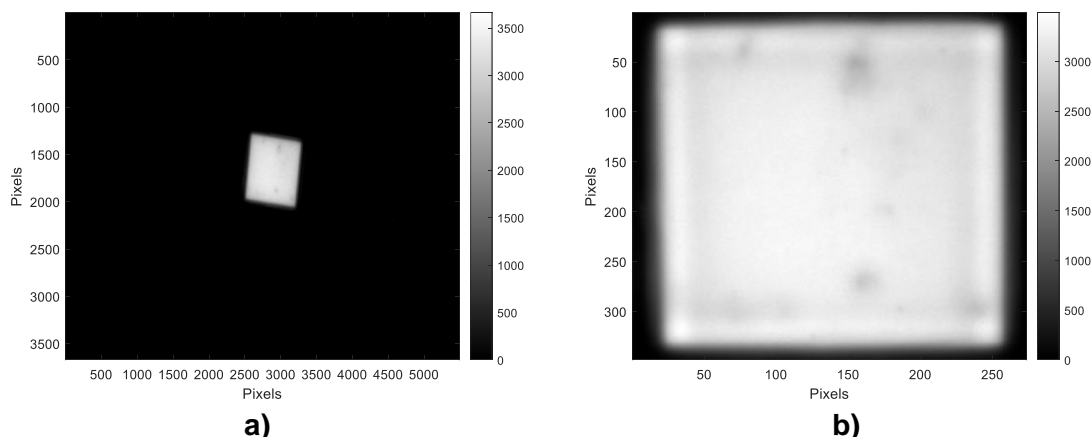


Figure 10. a) EL images of the silicon concentrator without the filter and b) the EL image after applying the correction routine.

The perovskite EL Images is shown in Figure 11.a), and the corrected image is Figure 11. b). The perovskite device consists out of six cells connected in series. Only three of the six is visible, indicating degradation has taken place in the bottom three cells as they are not optically active. The degradation is most likely due to moisture or oxygen ingress that occurred during outdoor exposure.

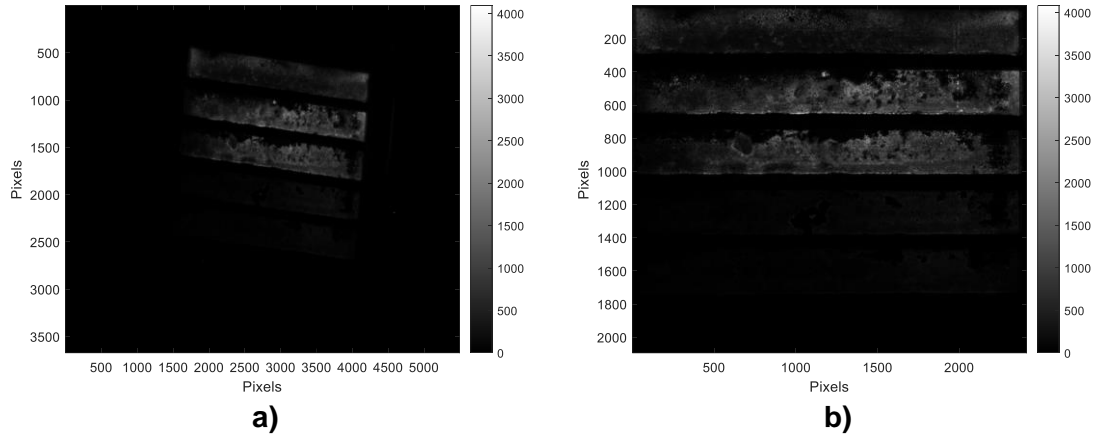


Figure 11. a) EL images of the perovskite solar cell and b) the EL image after applying the correction routine.

The EL image obtained for both the first and second layers of the Multi-junction III-V concentrator is shown by Figure 12.a) and Figure 13.a) respectively. The corrected images obtained from these EL images are shown by Figure 12. b) and Figure 13. b).

The image quality for both corrected images is sharp, and any interesting features appear significantly clearer than those seen in the silicon images. The contrast in the two layers is interesting to note as the top layer has a brighter perimeter whereas the second layer has a darker perimeter. This is likely related to the opto-electrical coupling between the layers. Two interesting features are highlighted in Figure 12.b) and Figure 13.b) with coloured rings. The feature highlighted by the blue ring is only seen in the top layer and not in the second layer. Whereas the feature highlighted by the red ring is only seen in the second layer and appears brighter in the first layer. This illustrates that these features are a characteristic of that specific layer of the Multi-junction III-V concentrator.

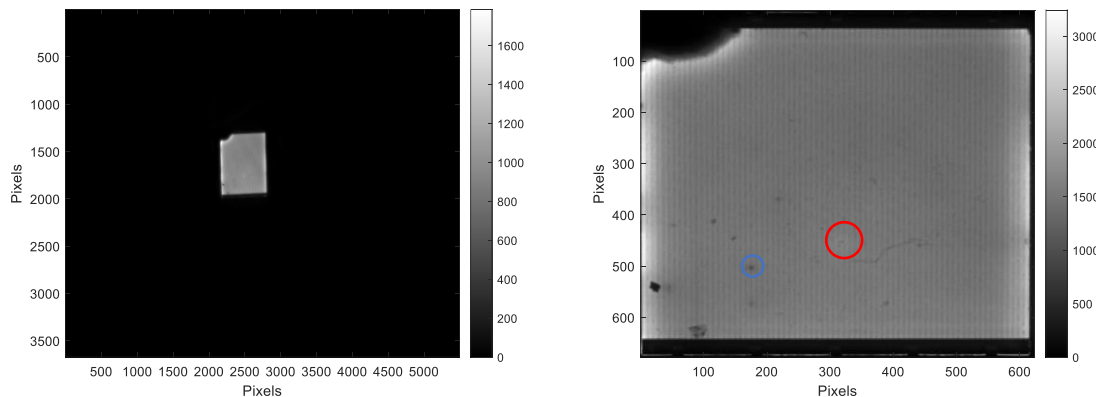


Figure 12. a) EL images of the First layer of the Multi-junction III-V concentrator and b) the EL image after applying the correction routine.

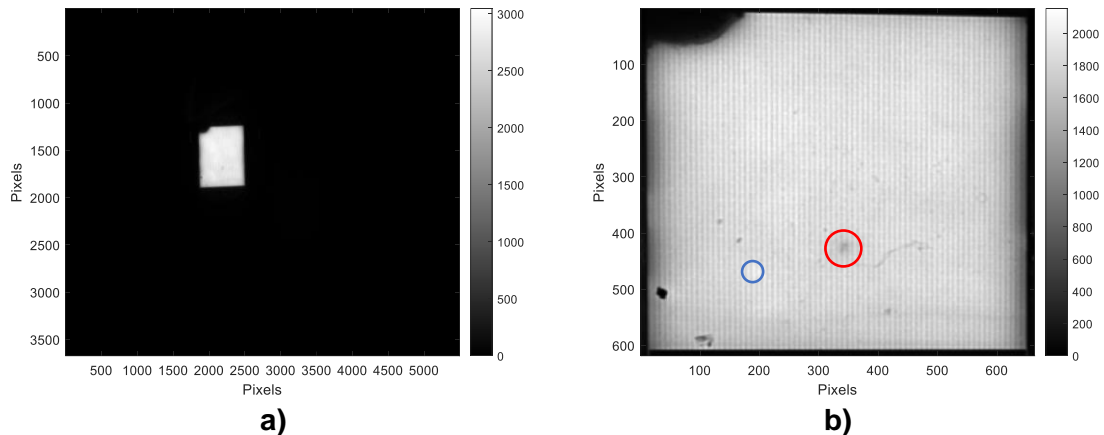


Figure 13. a) EL images of the Second layer of the Multi-junction III-V concentrator and b) the EL image after applying the correction routine.

5. Conclusions

In this paper an image correction routine was investigated for the applicability to other PV devices aside from silicon PV devices using a silicon CCD camera. It was found that imaging silicon PV devices with a filter in front of the CCD sensor yields higher quality images. Furthermore, it was found that the image correction procedure improves the quality of the images for not only Si cells but other technologies such as the MJSCs and perovskite PV cells. The incorporation of an appropriate PSF in the image correction routine for different PV technology devices will be used in future EL and PL image analysis to be conducted in our laboratory.

References

- Bedrich, K.G., Bliss, M., Betts, T.R. and Gottschalg, R. (2016), "Electroluminescence imaging of PV devices: Camera calibration and image correction", *Conference Record of the IEEE Photovoltaic Specialists Conference*, Vol. 2016-November, Institute of Electrical and Electronics Engineers Inc., pp. 1532–1537.
- Bliss, M., Wu, X., Bedrich, K.G., Bowers, J.W., Betts, T.R. and Gottschalg, R. (2015), "Spatially and spectrally resolved electroluminescence measurement system for photovoltaic characterisation", *IET Renewable Power Generation*, Vol. 9, Institution of Engineering and Technology, pp. 446–452.
- Bojek, P. (2022), "Solar PV, IEA (2022)", <https://www.iea.org/reports/solar-pv>, September.
- Breitenstein, O., Fruhauf, F. and Teal, A. (2016), "An Improved Method to Measure the Point Spread Function of Cameras Used for Electro- and Photoluminescence Imaging of Silicon Solar Cells", *IEEE Journal of Photovoltaics*, IEEE Electron Devices Society, Vol. 6 No. 2, pp. 522–527.
- Hameiri, Z., Mahboubi Soufiani, A., Juhl, M.K., Jiang, L., Huang, F., Cheng, Y.B., Kampwerth, H., *et al.* (2015), "Photoluminescence and electroluminescence imaging of perovskite solar cells", *Progress in Photovoltaics: Research and Applications*, John Wiley and Sons Ltd, Vol. 23 No. 12, pp. 1697–1705.
- Mitchell, B., Weber, J.W., Walter, D., MacDonald, D. and Trupke, T. (2012), "On the method of photoluminescence spectral intensity ratio imaging of silicon bricks: Advances and limitations", *Journal of Applied Physics*, Vol. 112 No. 6, available at: <https://doi.org/10.1063/1.4752409>.
- Payne, D.N.R., Juhl, M.K., Pollard, M.E., Teal, A. and Bagnall, D.M. (2016), "Evaluating the accuracy of point spread function deconvolutions applied to luminescence images", *Conference Record of the IEEE Photovoltaic Specialists Conference*, Vol. 2016-November, Institute of Electrical and Electronics Engineers Inc., pp. 1585–1589.

- Streetman, B. (1995), *SOLID STATE ELECTRONIC DEVICES*, Fourth Edition., Prentice-Hall International Editions.
- Trupke, T., Pink, E., Bardos, R.A. and Abbott, M.D. (2007), "Spatially resolved series resistance of silicon solar cells obtained from luminescence imaging", *Applied Physics Letters*, Vol. 90 No. 9, available at: <https://doi.org/10.1063/1.2709630>.
- Walter, D., Fell, A., Franklin, E., MacDonald, D., Mitchell, B. and Trupke, T. (2014), "The impact of silicon CCD photon spread on quantitative analyses of luminescence images", *IEEE Journal of Photovoltaics*, Vol. 4 No. 1, pp. 368–373.
- Würfel, P., Trupke, T., Puzzer, T., Schäffer, E., Warta, W. and Glunz, S.W. (2007), "Diffusion lengths of silicon solar cells from luminescence images", *Journal of Applied Physics*, Vol. 101 No. 12, available at: <https://doi.org/10.1063/1.2749201>.